Mechanism of Surface Modification of the Ti-6Al-4V Alloy Using a Gas Tungsten Arc Heat Source

M. LABUDOVIC, R. KOVACEVIC, I. KMECKO, T.I. KHAN, D. BLECIC, and Z. BLECIC

The surface modification of a Ti-6Al-4V alloy using a gas tungsten arc, as a heat source, was studied. The experimental results show that the titanium alloy surface can be melted and nitrided using pure nitrogen or a nitrogen/argon mixture shielding atmosphere. The resolidified surfaces are 0.9 to 1.2-mm thick and contain titanium nitride dendrites, α-titanium, and α''-titanium (martensite). The average dendrite arm spacing is influenced by the electrode speed. Small titanium nitride dendrites are homogeneously distributed in the resolidified surfaces. The microstructure and phase constitution in the resolidified surfaces were determined and analyzed, and the mechanism of the formation of titanium nitrides is discussed. The results show that the nitriding kinetics obey parabolic laws and are, therefore, controlled by nitrogen diffusion. The nitrogen-concentration depth profiles, calculated using Fick's second law of diffusion, are compared to experimental nitrogen depth profiles, showing satisfactory agreement.

I. INTRODUCTION

TITANIUM alloys have many attractive properties, including high specific strength and moduli, arising from their relatively low density, and their excellent corrosion resistance, primarily due to the formation of a passivating oxide film on the surface of the alloy. These properties have led to the use of titanium alloys in aerospace applications and in corrosive environments, but titanium alloys have found little use in general engineering applications. The main technological reason for this lack of engineering use is their poor wear resistance.

The literature reveals that a range of surface engineering techniques have been applied to titanium alloy substrates, including conventional thermochemical processes such as carburizing, nitriding, and boronizing, all of which were developed approximately 40 years ago.[1] However, these thermochemical processes have only met with limited success because of long treatment times, high temperatures, and nonuniformity of surface microstructure.[2] In addition, problems associated with poor ductility and significant reductions in fatigue limit have also been reported in the literature.[3]

Processes which create a gaseous discharge using nitrogen or ammonium gases, *e.g.*, plasma nitriding, have reduced the processing times involved[4] and also lowered the temperatures experienced at the surface from about 1000 °C to 400 °C,[5] thereby reducing some of the problems experienced using conventional nitriding techniques.

Other methods which involve the deposition of hard coatings (*e.g.*, CrN and TiN) by physical and chemical vapor-phase processes have a tendency to result in failure at the interface between the coating and the substrate, which leads to eventual loss of the coating on applied contact stresses.[6]

M. LABUDOVIC, R. KOVACEVIC, and I. KMECKO, are with the Department of Mechanical Engineering, Southern Methodist University, Dallas, TX 75275. T.I. KHAN is with the Department of Materials Engineering, Brunel University, Middlesex UB8 3PH, United Kingdom. D. BLECIC and Z. BLECIC are with the Faculty of Metallurgy and Technology, 81000 Podgorica, Yugoslavia.

Manuscript submitted August 4, 1998.

Recently, surface melting techniques have been developed utilizing lasers, where surface alloying is performed under a nitrogen gas shield.[7–13] Although it is an expensive alternative, an improvement in the wear resistance of titanium surfaces has been observed, but with some cracking in the laser-nitrided layers being reported.[10] However, Morten *et al.*[12] showed that this surface cracking could be eliminated by preheating the substrate before laser melting. This has the effect of reducing the steep temperature gradients and, therefore, the thermal stresses generated during laser processing.

Alternative heat sources, which can provide melting, such as an arc generation between a nonconsumable electrode and the substrate surface, are being used, for instance, in fusion-welding processes, to join materials. However, because these techniques have not been developed for surface engineering purposes, they remain untested as methods for surface modification. Therefore, this study is an extension of earlier work,[14] which has shown that, by using a gas tungsten arc heat source, surface melting of a Ti-6Al-4V alloy can be performed in a controlled atmosphere of pure nitrogen or in a mixture of nitrogen and argon to produce wear-resistant surfaces with hardness values (HV) greater than 900 $HV_{0.5}$. In this article, the effect of the processing parameters on the microstructural developments in the titanium alloy surface are presented.

II. EXPERIMENTAL PROCEDURE

The Ti-6Al-4V alloy was cut into rectangular plates (50 × 20 × 10 mm) and the surface was prepared to give a flat, polished finish, followed by a degreasing treatment in acetone before surface melting. An electrical arc was created between the nonconsumable tungsten electrode (3 mm in diameter) and the titanium alloy surface. An electrode negative polarity was used to provide good surface heating. An arc was produced by adjusting the distance between the tip and alloy surface and by careful control of parameters such as the current and voltage supply to the electrode. Shielding gases were channeled through the electrode holder, and gas flow regulators were used to control the flow rate to give a

mixture of argon and nitrogen, or pure nitrogen, as a gas shield. The electrode travel speed was varied between 4.17×10^{-3} m/s and 6.25×10^{-3} m/s using a four-axis positioning system.

The treated specimens were sectioned using a microtome low-speed cutter, so as to minimize the likelihood of any change in microstructure or hardness due to the cutting operation. The polished surfaces were etched using Kroll's reagent, and the microstructure, phase constitution, and chemical composition were examined using light microscopy, scanning electron microscopy, X-ray diffraction (XRD), and energy-dispersive spectroscopy (EDS). The nitrogen-concentration depth profiles were determined by the use of secondary ion mass spectroscopy (SIMS).

III. RESULTS AND DISCUSSION

A. *Effect of Surface-Modification Parameters on TiN Formation and Phase Constitution*

The arc current, arc interaction time, gas flow rate, pre- and postgas flow, electrode travel speed, and the composition of the shielding atmosphere must be carefully coupled and adjusted to obtain TiN in the microstructure of the titanium alloy surface. The effect of varying the composition of the shielding atmosphere and electrode travel speed on the formation of TiN at the surface can be seen in Table I. The results show that, in order to induce the formation of TiN in the surface, at a constant arc current, the nitrogen content of the shielding gas must be above 80 pct.

The electrode travel speed is found to effect the depth of the nitrided zone (Figure 1). This is because once the nitrogen gas has dissociated to produce a plasma, the speed will determine the time for which the surface is in contact with the plasma of nitrogen ions. The slower the speed, the greater the time for diffusion of ions into the molten surface.

The modified surfaces were studied in detail by diffraction, using Cu K_α and Mo K_α X-rays. The two different kinds of X-rays penetrate to different depths, and each, therefore, gives information about the phase constitution at different depths below the surface. The X-ray penetration depth in titanium for Cu K_α is about 25 μm, while the penetration depth for Mo K_α X-rays is about 216 μm. In both cases, the main phases identified were TiN and α-titanium. However, when the cross sections of the surfaces are studied using Cu K_α X-rays, a mixture of TiN, α-titanium, and α''-titanium (martensite) was identified in the middle of the resolidified surfaces (Figure 2). The β-titanium is transformed to α''-titanium (martensite) due to rapid cooling.

The microstructural developments within the various microzones of the resolidified regions are shown in Figure 3. TiN dendrites were observed at a distance of about 0.3 mm from the surface (Figure 3(a)). A microstructure of α''-titanium (martensite) is shown in Figure 3(b). A mixture of titanium nitride, α-titanium, and α''-titanium (martensite) is shown in Figure 3(c). The total depth of the resolidified region is between 0.9 and 1.2 mm. Porosity and cracking in the titanium-nitrided layer was not observed.

The structure of TiN has been investigated extensively in

Table I. The Impact of Process Parameters (Electrode Travel Speed and the Composition of Shielding Atmosphere) on the Production of TiN

Specimen Number	Current (A)	Shielding Atmosphere	Electrode Travel Speed (mm/s)	TiN
1	110	20 pct N_2/80 pct Ar	4.17	no
2	110	20 pct N_2/80 pct Ar	5.00	no
3	110	20 pct N_2/80 pct Ar	6.25	no
4	110	50 pct N_2/50 pct Ar	4.17	no
5	110	50 pct N_2/50 pct Ar	5.00	no
6	110	50 pct N_2/50 pct Ar	6.25	no
7	110	80 pct N_2/20 pct Ar	4.17	yes
8	110	80 pct N_2/20 pct Ar	5.00	yes
9	110	80 pct N_2/20 pct Ar	6.25	yes
10	112	100 pct N_2	4.17	yes
11	112	100 pct N_2	5.00	yes
12	112	100 pct N_2	6.25	yes

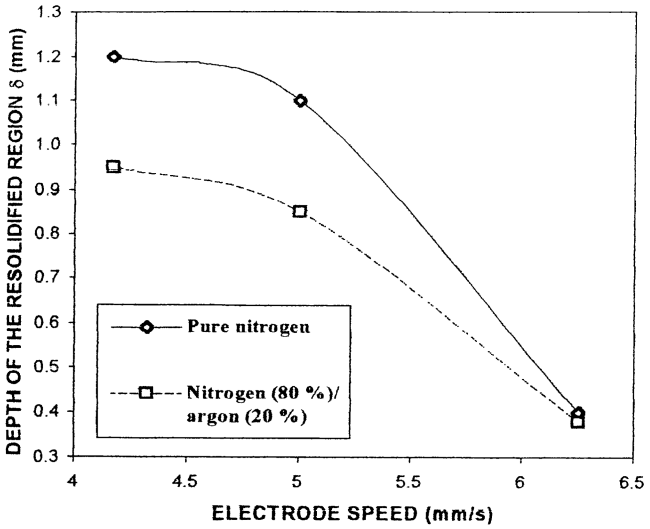

Fig. 1—The influence of the electrode travel speed on the depth of the modified surfaces treated under a pure nitrogen or a nitrogen/argon mixture gas shield.

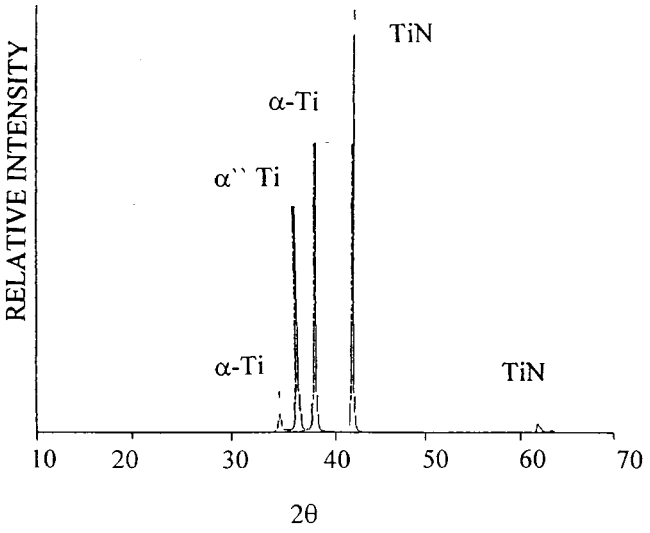

Fig. 2—X-ray analysis of the cross section of the modified surface treated under a pure nitrogen gas shield (center of the resolidified region).

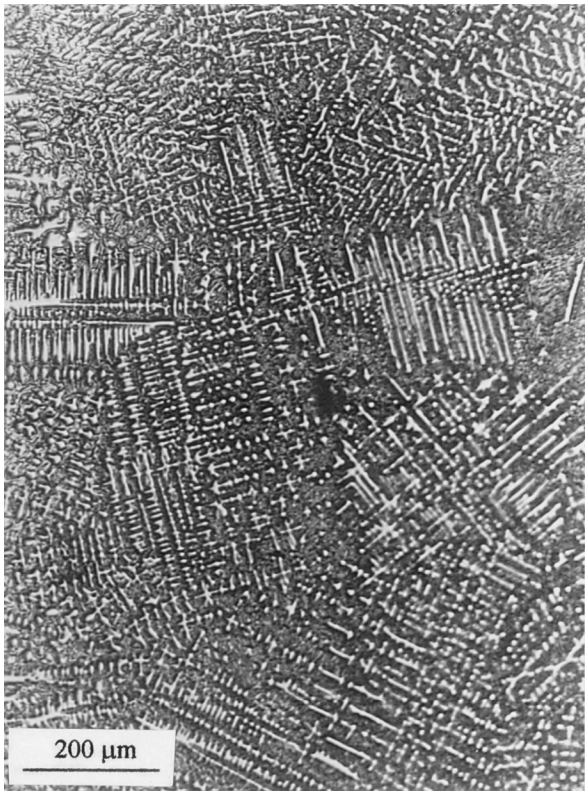

(*a*)

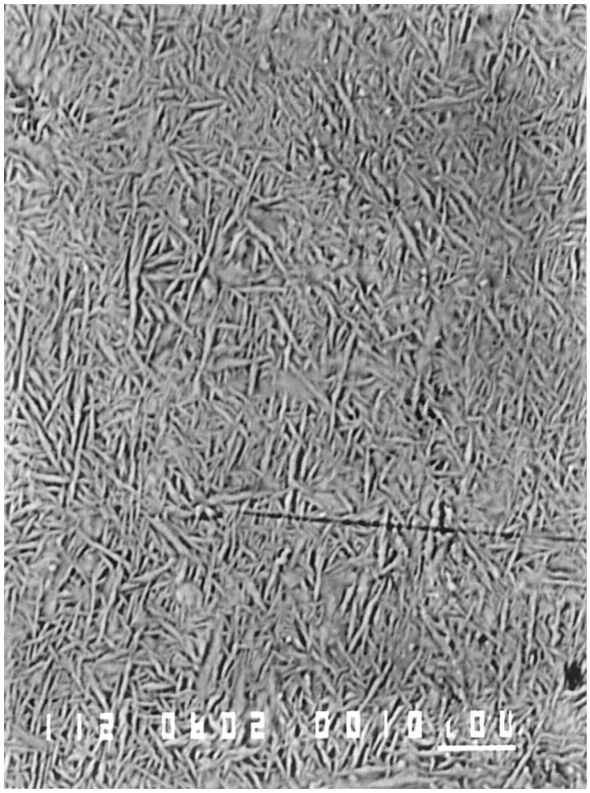

(*b*)

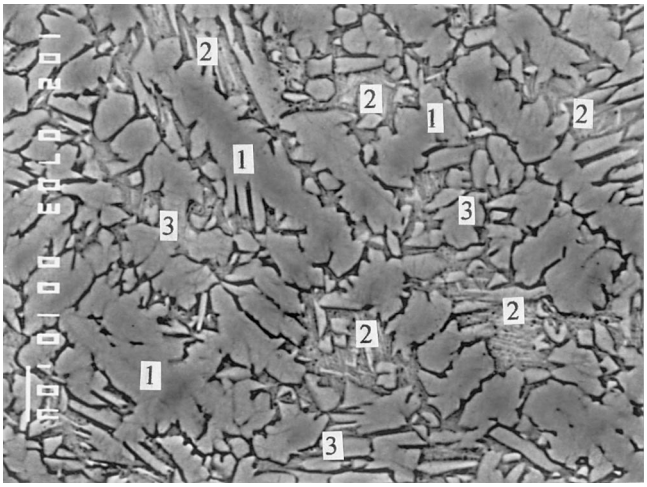

1-TiN; 2-α''-titanium (martensite); 3-α-titanium.

(*c*)

Fig. 3—The microstructure of the resolidified region: (a) 0.1 mm from the surface (edge of the resolidified region); (*b*) 0.8 mm from the surface (end of the resolidifed region); and (*c*) 0.5 mm from the surface (center of the resolidified region).

the past,[15,16] and is shown to have an fcc structure with a lattice parameter (*a*) value of 4.232 A when the ration of N/Ti is equal to unity.[17] In this article, the least-mean-squares method was used for the calculation of the lattice parameters of TiN from the XRD data, and the results are shown in Figure 4. It can be seen that the lattice parameters affected by the content of nitrogen in TiN. In addition, when the nitrogen content in the shielding atmosphere changes from 80 to 100 vol pct, the lattice parameter increases, but the increase is small, from 4.226 to 4.238 A on average. This increase in the lattice parameter is considered to be due to an effect of the tensile residual stresses generated on rapid cooling.

The influence of the electrode travel speed and the composition of the shielding atmosphere on the secondary dendrite arm spacing is shown in Figure 5. From the results, it is clear that the dendrite arm spacing is influenced by the shielding gas composition and the electrode travel speed used. The secondary dendrite arm spacing is lower when melting under pure nitrogen gas rather than under a mixture of argon/nitrogen gas. Normally, one would find decreasing secondary dendrite arm spacing with an increasing electrode

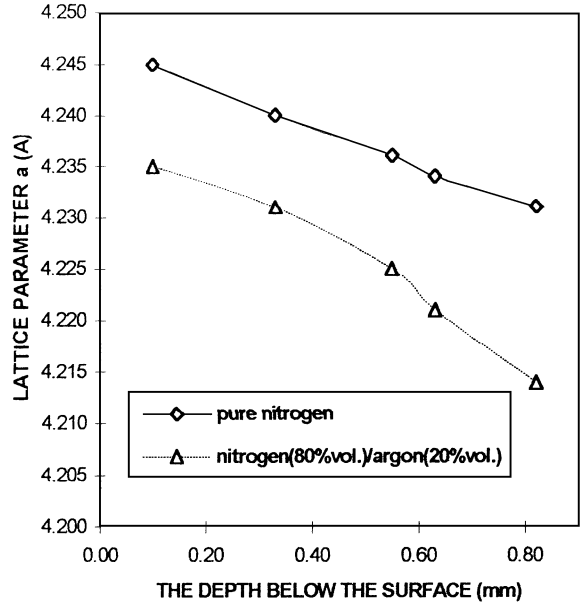

Fig. 4—The dependence of the lattice parameter *a* of TiN on the depth below the surface of the Ti-6Al-4V treated under a pure nitrogen or a nitrogen/argon mixture gas shield.

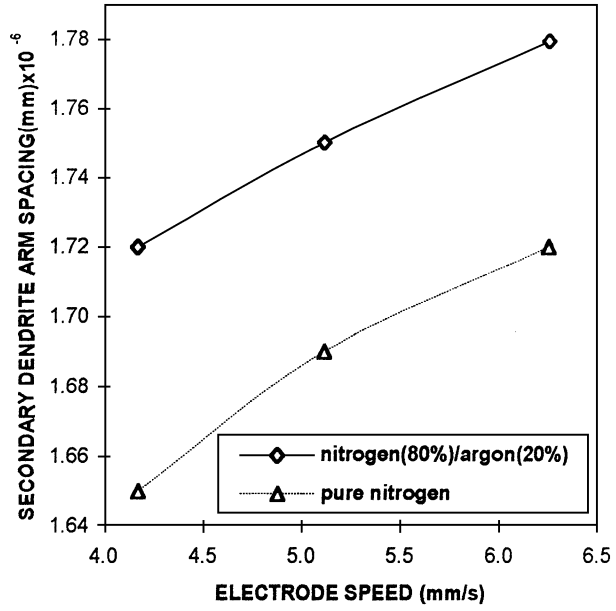

Fig. 5—Relationship between secondary dendrite arm spacing and electrode travel speed for different compositions of shielding atmosphere.

travel speed. However, in this case, as the electrode travel speed decreases, more refinement in the microstructure was observed, resulting in a decrease in secondary dendrite arm spacing. It appears that greater nitrogen pickup in the molten metal significantly decreases the secondary dendrite arm spacing. In this case, the slower electrode travel speed simply increases the nitrogen content of the metal substantially and, thereby, affects the cooling rate and refines the microstructure directly.

This change in microstructure is a function of the cooling rate. When nitrogen is used, a steep temperature gradient is established across the solid/liquid interface, because nitrogen, being a diatomic gas, is capable of transferring a greater amount of energy than monoatomic gases such as argon. Therefore, the heat input to the surface is significantly greater than that for the argon/nitrogen mixture, which, in turn, increases the cooling rate.

B. *Titanium Nitriding Kinetics*

The chemical composition of the resolidified surfaces was determined by EDS, and the analyses are listed in Table II. It can be seen that the chemical composition varies with depth below the resolidified titanium alloy surface.

Three chemical reactions may be involved during surface modification of the titanium alloy using a gas tungsten arc as a heat source. The Gibbs free energies for possible nitride-forming reactions are shown in Table III. This comparison shows that vanadium nitride is unlikely to form because of its positive Gibbs free-energy value, but nitrides of titanium and aluminum could be expected to form in the surface. The values of the equilibrium partial pressures of individual elements over liquid Ti-6Al-4V, calculated assuming ideal solution behavior at 2000 and 2500 K, are presented in Table IV. It is observed from the calculated values that the extent of variation in the equilibrium partial pressures resulting from the change in temperature is different for individual elements. Since the vaporization rates of the individual elements are proportional to their equilibrium partial pressures, selective vaporization of aluminum may be very strong during melting of Ti-6Al-4V. Therefore, a decrease in aluminum content would be expected after surface melting, which is observed in the compositional analysis of the resolidified surfaces shown in Table II. As a result, TiN formation will be the dominant reaction on surface modification.

When titanium nitride is cooled slowly, according to the Ti-N equilibrium-phase diagram, TiN can transform into Ti_2N. However, during arc melting of the surface, a cooling rate of 7.62×10^4 K/s is calculated from the TiN secondary dendrite arm spacing using the following relationship:

$$\lambda = B(GR)^{-n}$$

where G is the thermal gradient and R is the solidification velocity. The constants were given values of $B = 80.9$ and $n = 0.34$ for the titanium alloy.[17] Under this condition, the reaction $TiN \rightarrow Ti_2N$ is inhibited during supercooling. If TiN (NaCl structure) transforms into Ti_2N (TiO_2 structure), the reaction involves not only a structural transformation, but also a change in composition. Therefore, under supercooling conditions, the reaction $TiN \rightarrow Ti_2N$ is not favored, and the mechanism of surface modification of a Ti-6Al-4V alloy using a gas tungsten arc heat source can be described by the following reaction sequence:

(1) surface adsorption: $[Ti] + N_2 \rightarrow [Ti] + [N_2]$;

(2) nitrogen decomposition: $[N_2] \rightarrow 2N$;

(3) nitrogen diffusion: $[N]_{surface} \rightarrow [N]_{inside}$;

(4) TiN precipitation: $[Ti(N)] \rightarrow TiN + [Ti(N)]'$; and

(5) melt solidification: $[Ti(N)]' \rightarrow TiN + \alpha\text{-Ti(N)}$.

where [] refers to a liquid solution and (N) represents N in the titanium alloy surface.

The kinetic curves of the nitrided-layer thickness (δ) changes with time (τ), for different mixtures of shielding

Table II. Chemical Composition of the Resolidified Region

Number	Chemical Composition (Wt Pct)				Place Measured
	Ti	Al	V	N	
1	49.15	—	1.64	49.21	0.1 mm from the surface
2	50.59	1.32	3.67	44.42	0.2 mm from the surface
3	49.18	6.08	4.54	40.20	0.4 mm from the surface
4	59.37	—	2.01	38.62	center of the resolidified region
5	60.22	—	2.34	37.44	edge of the resolidified region
6	65.26	0.52	4.04	30.18	end of the resolidified region

Table III. The Gibb's Free Energies (ΔG) for Various Reactions

Reaction	Gibb's Energy (J/mol)			
	T = 1700 K	T = 1900 K	T = 2100 K	T = 2300 K
$Ti + N_2 \rightarrow 2TiN$	-7.70×10^5	-5.50×10^5	-4.70×10^5	-3.60×10^5
$Al + N_2 \rightarrow 2AlN$	-4.70×10^5	-3.80×10^5	-2.60×10^5	-14.20×10^4
$V + N_2 \rightarrow 2VN$	-2.50×10^4	2.50×10^4	11.80×10^4	18.40×10^4

Table IV. The Partial Pressures for Aluminum, Vanadium, and Titanium

Element	Concentration (Wt Pct)	Partial Pressure (Pa)	
		T = 2000 K	T = 2500 K
Al	6	74.00	2.10×10^3
Ti	90	7.70×10^{-1}	1.70×10^2
V	4	6.00×10^{-3}	3.20

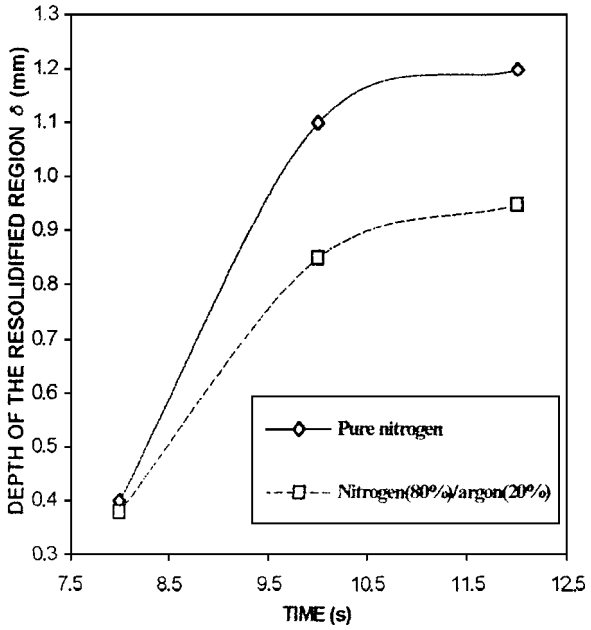

Fig. 6—Kinetics curves of nitrided layer thickness changes with time for different composition of shielding atmosphere.

atmospheres, are presented in Figure 6. The results show that nitriding kinetics follow a parabolic growth law within the investigated range of treatment time, which can be expressed as

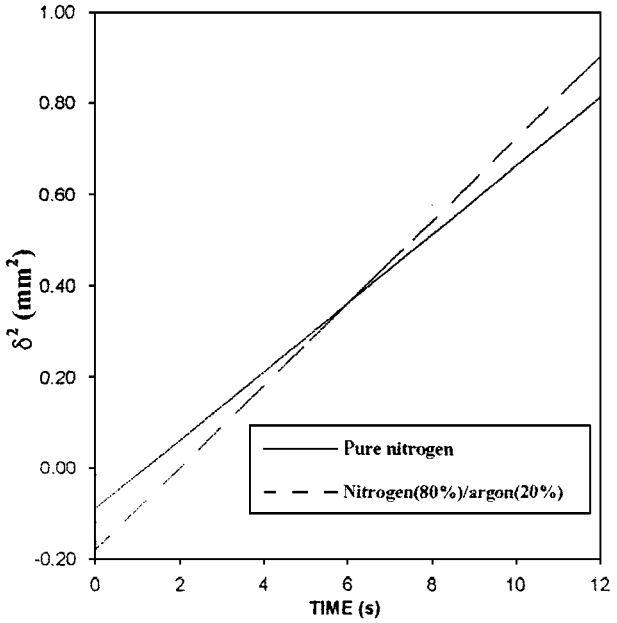

Fig. 7—Determination of parabolic rate constant (K') and integration constant (A).

$$d\delta/d\tau = K'/\delta \quad [1]$$

where K' is the parabolic rate constant.

The titanium-nitriding kinetics are, therefore, controlled by the diffusion of nitrogen from the surface to the interior of the material (reaction 3).

Integrating Eq. [1], it follows that

$$\delta^2 = 2K'\tau + A \quad [2]$$

where A is the integration constant.

By the use of Eq. [2], the curves in Figure 4 are linearized in the (δ^2 and τ) coordinate system (Figure 7). Then, from Figure 7, by the use of linear regression analysis, the average value of K' and the integration constant A are calculated:

$$K' = 0.047 \text{ mm}^2/\text{s}$$

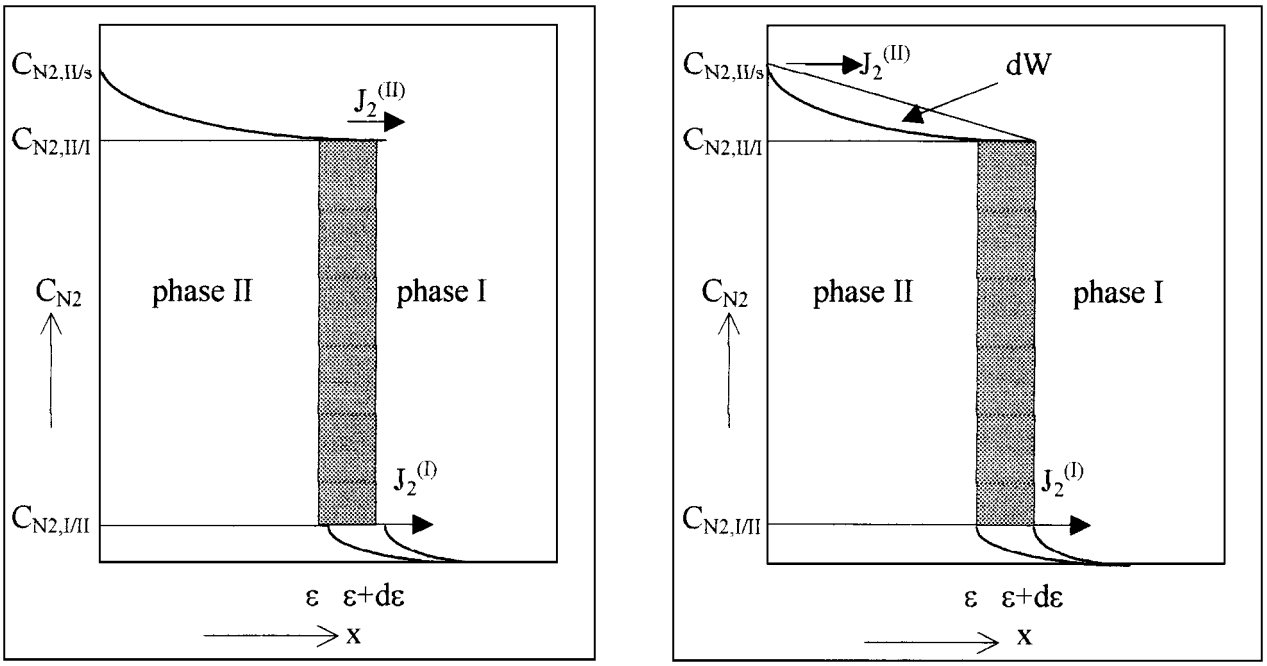

(*a*) (*b*)

Fig. 8—Schematic concentration-depth profile: (*a*) to illustrate Eq. [4] and (*b*) to illustrate Eq. [5].

$$A = -0.14 \text{ mm}^2$$

Inserting these values in Eq. [2], the kinetics growth rate can be expressed as

$$\delta^2 = 0.094\ \tau - 0.14 \qquad [3]$$

C. *Determination of the nitrogen diffusion coefficient*

From the evolution of the nitriding layer's thickness with time (Figure 6), the nitrogen diffusion coefficient can be determined by solving Fick's second law, in the case of monolayer growth, with one diffusion component. A mathematical description for the determination of the diffusion coefficient is as follows.

In the situation given in Figure 8(a), phases I (titanium alloy substrate) and II (TiN layer) are composed of components 1 and 2. Component 2 (solute N) is assumed to be mobile and to dissolve in both phases I and II, while component 1 (solvent Ti) is assumed to be immobile. At the surface, the concentration of solute atoms of component 2(N) is denoted by $C_{N2,II/S}$. At the layer substrate interface, the solute concentration decreases to $C_{N2,II/I}$ in phase II and to $C_{N2,I/II}$ in phase I. For shifting the interface between the layer and substrate (ε) an infinitesimal distance ($d\varepsilon$) into the substrate within an infinitesimal lapse of time ($d\tau$), an amount of $(C_{N2,II/I} - C_{N2,I/II})d\varepsilon$ of component 2 is used (shaded area in Figure 8(a)). Then, the following continuity equation holds:

$$\begin{aligned}(C_{N2,II/I} - C_{N2,I/II})d\varepsilon &= (J_2^{(II)}{}_{(x\varepsilon)} - J_2^{(I)}{}_{(\varepsilon x)})\ d\tau \\ &= [(-D_{N2}^{(II)}\ dC_{N2}/dx)_{(X\varepsilon)} \\ &\quad - (-D_{N2}^{(I)}\ dC_{N2}/dx)_{(\varepsilon x)}]\ d\tau\end{aligned} \qquad [4]$$

where $J_2^{(k)}$ is the flux of component 2(N) in phase k, dC_{N2}/dx is the concentration gradient of the diffusing component 2(N), and $D_{N2}^{(k)}$ is the diffusivity of component 2(N) in phase k.

Alternatively, for a layer growing into a substrate, growth of the layer can be expressed in terms of the flux of component 2(N) entering the layer at the surface and the flux of component 2(N) leaving the layer at the interface (Figure 8(b)). Then, the continuity equation for growth of the layer (shaded area in Figure 8(b)) becomes

$$\begin{aligned}(C_{N2,II/I} - C_{N2,I/II})\ d\varepsilon + dW &= (J_2^{(II)}{}_{(x=0)} - J_2^{(I)}{}_{(\varepsilon x)})\ d\tau \\ &= [(-D_{N2}^{(II)} dC_{N2}/dx)_{(x=0)} \\ &\quad - (-D_{N2}^{(I)} dC_{N2}/dx)_{(\varepsilon x)}]\ d\tau\end{aligned} \qquad [5]$$

where dW is the amount of solute N accumulated in the layer to maintain a concentration-depth profile (Figure 8(b)).

Equations [4] and [5] are equally valid descriptions for layer-growth kinetics. If the mass increase of a specimen is monitored to investigate layer growth, Eq. [5] should be used rather than Eq. [4], because the mass-increase rate is directly related to the flux of component 2(N) entering the specimen. To assess the diffusion coefficient $D_{N2}^{(II)}$ from Eqs. [4] or [5], the value for the corresponding concentration gradient should be known. Moreover, employing Eq. [5] requires that the value of dW be known. Both parameters (dC_{N2}/dx and dW) could be calculated simply if the concentration-depth profile within the layer is known. Solving Fick's second law, for a known or an assumed concentration dependency of the diffusion coefficient and the appropriate boundary conditions, provides this concentration-depth profile. For this purpose, we used an analytical solution of Fick's second law, as used previously by Debuigne[18] for the oxidation of zirconium and by Bars *et al.*[19] for titanium nitriding.

From this point, we calculated the evolution of the atomic percentage of nitrogen with the substrate depth using Fick's second law and determined the diffusion coefficient of nitrogen,

$$D = 4.40 \times 10^{-4} \text{ cm}^2/\text{s}$$

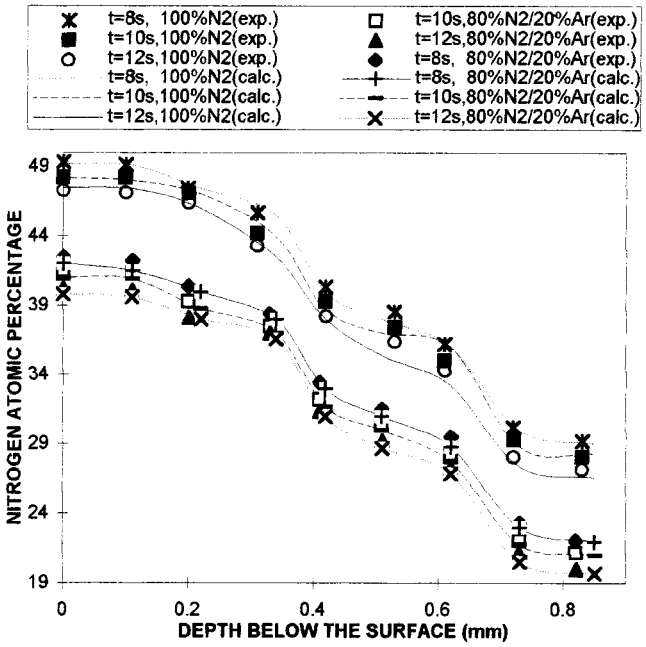

Fig. 9—Distribution of calculated and measured nitrogen atomic percentages with depth for different compositions of shielding atmosphere.

In Figure 9, the calculated nitrogen-concentration depth profiles have been compared to those measured experimentally by SIMS. The part of Figure 9 corresponding to the depth between 0.3 and 0.5 mm from the surface is calculated using the least-squares method to fit the measured concentration dependence with calculated ones, in order to infer a diffusion coefficient from those data. The discrepancies between measured and calculated values for these data may result from liquid stirring. However, satisfactory agreement has been obtained for the rest of the data.

IV. CONCLUSIONS

This study has shown that the modified surfaces are comprised of distinct phase distributions. The resolidified surface region consists primarily of TiN and α-Ti, followed by a zone showing a mixture of TiN + α-Ti + α''-Ti. The average size of the TiN dendrites is affected both by the composition of the shielding gas used and the electrode travel speed. When nitrogen gas is used, a fine dendrite microstructure is achieved, and this is attributed to the faster cooling rates achieved than with the argon/nitrogen mixture. As the electrode travel speed is increased during surface melting, a corresponding increase in dendrite spacing is recorded.

The kinetics of titanium nitriding follows a parabolic growth rate and, therefore, is controlled by nitrogen diffusion. The nitrogen-concentration depth profiles calculated using Fick's second law show satisfactory agreement with experimental nitrogen-concentration depth profiles.

REFERENCES

1. R. Hanzell: *Met. Progr.*, 1954, vol. 65, p. 89.
2. R.A. Rowntree: *2nd Eur. Space Mechanisms and Tribology Symp.*, Conf. Proc, J.L. Murray, Ed., Meersburg, 1985, pp. 167-71.
3. E. Mitchell and P. Brotheron: *J. Inst. Met.*, 1964–1965, vol. 93, p. 381.
4. H.J. Brading: Ph.D. Thesis, University of Birmingham, Birmingham, 1992.
5. M. Miyagi, Y. Sato, T. Mizuno, and S. Sawada: *Titanium '80, 4th Int. Conf. on Titanium*, Conf. Proc., TMS-AIME, Warrendale, PA, 1980, vol. 4, p. 2867.
6. J.A. Davidson and A.K. Mishra: *Surface Modification Technologies V*, Conf. Proc., T.S. Sudarshan and J.F. Braza, eds., Institute of Materials, Birmingham, 1992, p. 1.
7. M. Salehi, T. Beil, and P.H. Morten: *Surface Modification Technologies IV*, Conf. Proc., TMS, Birmingham, 1991, pp. 991-1002.
8. S. Yeramaredddy and S. Bahadur: *Wear*, 1992, vol. 157, p. 245.
9. O.V. Akgun and O.T. Inal: *J. Mater. Sci.*, 1994, vol. 29, p. 1159.
10. H. Xin, S. Mridha, and T.N. Baker: *J. Mater. Sci.*, 1996, vol. 31, p. 22.
11. P.H. Morten, T. Bell, A. Weisheit, J. Kroll, B. Mordike, and K. Sagoo: *Surface Modification Technologies V*, Conf. Proc., Institute of Materials, Birmingham, 1992, pp. 593-609.
12. W.M. Weerasinghe, D.R.F. West, and J. de Damborenea: *J. Mater. Processing Technol.*, 1996, vol. 58, p. 79.
13. B.L. Mordike: *Laser Surface Treatment of Metals*, Conf. Proc., C.W. Draper and P. Nazoldi, eds., Martinus Nijhoff, Dordrecht, 1986, pp. 451-60.
14. M. Labudovic and T.I. Khan: *J. Mater. Sci. Technol.*, 1998, vol. 14, p. 357.
15. R.A. Andrievskii, J.F. Khromov, D.E. Svitsunov, and R.S. Jurkova: *Russ. J. Phys. Chem.*, 1983, vol. 57, p. 996.
16. H.A. Wriedt and J.L. Murray: *Phase Diagrams of Binary Titanium Alloys*, Conf. Proc., J.L. Murray, ed., ASM INTERNATIONAL, Metals Park, OH, 1987, p. 176.
17. A.D. McQuillan and A.K. McQuillan: *Titanium*, Academic Press, New York, NY, 1956.
18. J. Debuigne: *Metaux Corrosion Industrie*, 1967, vol. 89, p. 499.
19. J.P. Bars, E. Etchessahar, and J. Debuigne: *J. Less Common Met.*, 1977, vol. 52, p. 51.